2019 International Conference on Robotics and Automation (ICRA)
Palais des congres de Montreal, Montreal, Canada, May 20-24, 2019

Automated Cell Patterning System with a Microchip using Dielectrophoresis

Kaicheng Huang, Henry K. Chu*, *Member, IEEE*, Bo Lu, Jiewen Lai and Li Cheng

***Abstract*— The ability to patterning cells is an important technique to facilitate cell-based assay and characterization. In this paper, an automated cell patterning system was developed for the fabrication of large-scale cell patterns. To resolve the challenge of the limited printable area, the cell-printing microchip and the substrate were mounted on the movable stages of the system, and large-scale cell patterns were realized through coordination between the stages. An autofocusing technique was integrated in the system to evaluate the gap between the microchip and the substrate. In order to enhance the performance of the patterning system, different experimental parameters, including the velocity of the moving stage, were examined. Yeast cells suspending in 6-aminohexanoic acid (AHA) solution were considered in this study, and a sequence of characters was successfully printed using the proposed system. The results confirm that this system offers an automatic method with high flexibility to construct large-scale cell patterns for various applications.**

I. INTRODUCTION

Cell is the basic unit of every biological creature [1]. With the extracellular matrix (ECM) support, cells can grow into a complex network that regulates various functions, including signal transport, information transmission and energy transfer. Therefore, the arrangement of cells on the ECM is very important so as to enable communication between cells from one end to the other. Using our native tissues as an example, cells are arranged in an organized manner, rather than randomly distributed on the ECM.

To arrange cells into a particular form, micromanipulation techniques can be utilized to drive cells to a particular position. Various techniques that are invasive to biological cells have been studied, and these include electrophoresis force manipulation [2], dielectrophoresis (DEP) force manipulation [3], magnetic force manipulation [4] and hydrodynamic force manipulation [5]. Among all, DEP force manipulation has widely been used for cell manipulation as it does not need any special treatment or reagent which could pose a hazard to the cells. The DEP phenomenon was firstly discovered by Pohl [6], where electrically neutral micro objects can be polarized in a non-uniform electric field, making non-contact manipulation by the electrical force. The strength of the DEP is dependent on the gradient of the electric field, and the direction is based on the electrical properties between the cell and the aqueous environment. If the cell is pulled to the high electric field area, it is called positive-dielectrophoresis (p-DEP). Conversely, the phenomenon that the cell is driven to the low electric field area is called negative-dielectrophoresis (n-DEP). DEP has been widely used in the biomedical research including sorting, separation, filtering, characterization and diagnosis. For patterning, several groups [7]–[9] have developed simple microchips to create line and dot patterns using cells. In addition, electrodes on the microchip can be switched on or off to manipulate cells from one position to another. Although these methods can create different cell patterns, there is a limitation that each microchip is uniquely designed for its intended application. The cell pattern is determined by the electrode configuration and many parameters, such as the size of the microchannel, cannot be changed after fabrication.

To improve the flexibility of the DEP technique, one stream of research is known as light-induced DEP. In this technique, a pair of photosensitive semiconductor is utilized as the electrodes. Upon illumination by a focused light beam, the electrical conductivity at the exposed region becomes higher, allowing electric fields to be generated. Through manipulating and controlling the beam to different positions, different cell patterns can be created. For instance, Grad et al. [10] employed optical beams as tweezers to handle non-adherent cells. Similarly, Huang et al. [11] used the optoelectronic tweezers to achieve single cell separation. Hsu et al. [12] fabricated a phototransistor-based DEP platform for dynamic cell manipulation. Miccio et al. [13] performed cell immobilization and orientation with the help of light-induced DEP. Although the light-induced DEP technique overcomes the restriction of traditional DEP, there are still some drawbacks to this technique. One of the most important problems is that the semiconductor (electrodes) and the suspending medium need be transparent for light penetration. Also, to reduce the complexity in setup, a single light source is commonly used to project a beam concurrently on both semiconductor, limiting the variation of electric fields to be generated within the environment. Hence, there remains a need for a more universal platform to facilitate DEP research for various applications.

In our previous work, we have developed a microchip which can generate ring-like electric fields to gather cells, creating a dot array on different substrates [14]. In this study, we extend the capability and the functionality of the microchip by integrating into a motorized microscope system. The microchip is mounted on a linear stage so that the height of the microchannel can be adjusted rather than attached on the substrate. By combining with the movable stage, the

The work was supported in part by the Research Grant Council of the Hong Kong Special Administrative Region, China, under Grant 25204016.

K. Huang, H. K. Chu*, B. Lu, J. Lai and L. Cheng are with the Department of Mechanical Engineering, The Hong Kong Polytechnic University, Hong Kong. (*Corresponding Author, email: henry.chu@polyu.edu.hk)

relative position between the substrate and the microchip can be precisely controlled so as to enable construction of large-scale cell patterns. In order to evaluate the feasibility of this system, a series of tests were conducted to examine the effect of different experimental parameters on this cell patterning system. After optimization, a large-scale cell pattern was created to demonstrate the performance of this system.

II. DESIGN OF THE SYSTEM

A. The microchip design

This multi-layer microchip employs the n-DEP technique, which creates non-uniform electric fields through different layers for cell manipulation. For dielectric particles, a net DEP force, $\boldsymbol{F}_{DEP}$, acting on the particles, can be evaluated as:

$$\boldsymbol{F}_{DEP} = 2\pi r^3 \varepsilon_m \cdot Re[K(\omega)] \cdot \bigtriangledown E^2 \tag{1}$$

where r is the particle radius, ε_m is the permittivity of the suspending medium, $\bigtriangledown$ is the Del vector operator, E is the root mean square of electric field and $Re[K(\omega)]$ is the real part of the Clausius-Mossotti (CM) factor:

$$K(\omega) = \frac{\varepsilon_p^* - \varepsilon_m^*}{\varepsilon_p^* + 2\varepsilon_m^*} \tag{2}$$

where ε_p^* is the complex permittivity of the particle and ε_m^* is the complex permittivity of the suspension medium.

For viable cells, a double-shell model introduced by Huang et al. [15] is proven to be appropriate to model the cell behaviours under the DEP phenomenon. Using a smeared-out approach, the complex permittivity of yeast cells as a homogeneous particle can be evaluated. According to the equation, the sign of the CM factor decides the direction of the DEP force, which is dependent on the electrical properties of the cell and the medium. However, these two properties are related to the application and cannot be changed. In contrast, the operating frequency of the input signal, ω, can be adjusted to determine the sign of the CM factor. To arrange and pattern cells onto the substrate, n-DEP force is required to pull the cells and the signal frequency in this work is set at above 6MHz to induce n-DEP force for cell manipulation.

The schematic diagram of the microchip is shown in Fig.1(B). The chip consists of 16 electrodes, with a diameter of $400\mu m$, that are arranged in a "4×4" manner. An electrode layer with 16 holes is served as the common electrode. Each electrode is connected to the function generator through an electrical relay, which can selectively turn on or off (shown in Fig.1(A)), to generate a ring-like electric field.

B. Design of the patterning system

The microchip design can effectively generate a ring-like electric field within a microenvironment to drive the surrounding cells toward the center of the electrode, and subsequently pattern onto the substrate. However, similar to typical microfluidic chips, it would be quite challenging to detach or separate the patterned substrate which is irreversibly bonded to the chip.

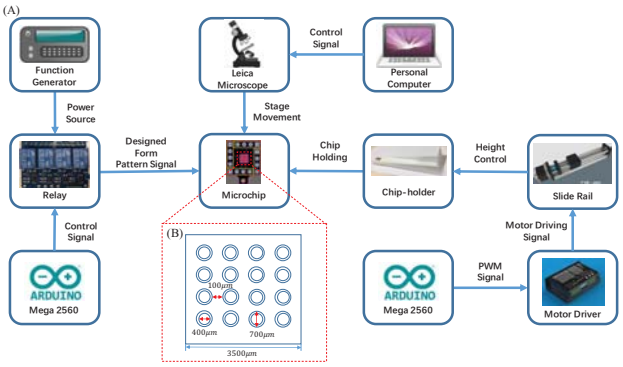

Fig. 1. The diagram of the system setup (A). The components of system (B). The schematic diagram of the microchip

In this work, an adjustable microenvironment is created between the substrate and the microchip through the use of a linear stage. According to the research by Ino et al. [7], the n-DEP effect would become negligible when the gap between the electrodes and substrate is larger than $100\mu m$. Hence, a gap distance of $100\mu m$ is considered in this study and the linear stage can provide motions for the microchip along with the optical axis of the microscope. The microchip is attached to the linear stage through a 3D printed chip-holder, and the position of the stage can be controlled by sending signals through the motor driver via an Arduino board. Since the linear stage has a total length of 30cm, the stage is secured on the anti-vibration table using screws, and two supporting girders are added to minimize vibration. The microscope system used for inspection is Leica DMi8 model. The microscope system is equipped with a motorized stage for positioning the glass substrate to the underneath of the microchip for cell patterning, and a motorized vertical stage to adjust the objective lens. A control interface was developed using C++ program, which can display images from the microscope to facilitate coordinated movements between the linear stage, the motorized stage, and the vertical stage. The complete setup of the automatic cell patterning system is shown in Fig.1.

C. Auto focusing system for chip positioning

The experiment requires the microchip to be located at $100\mu m$ above the glass substrate and an image-based method was adopted for height evaluation. The procedure of the microchip setting is shown in Fig.2(A)-(D). First, the objective lens is adjusted to focus on the surface of the glass slide, where the microscope image can show the cells adhered on the surface in focus. Then, the objective lens is repositioned to the focus at $100\mu m$ above the glass substrate. The linear stage was manipulated to bring the microchip towards the substrate surface. By continuously monitoring the microscope images, the linear stage will stop until the microchip appeared in the image is in focus. To judge whether or not the microchip is in focus, an auto-focusing method is employed to detect the sharpness of the image. The Laplacian operator is used to apply on the image to detect the gradients of the image, and the function is given

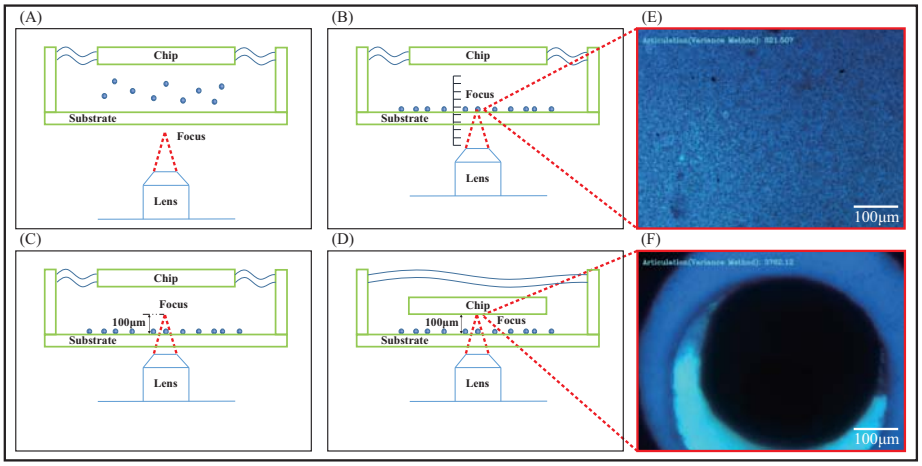

Fig. 2. (A)-(D). The procedure of chip setting (E). The image of the cell in focus (F). The image of the chip in focus

as:

$$\mathcal{L}(f) = \frac{\partial^2 f}{\partial x^2} + \frac{\partial^2 f}{\partial y^2} \tag{3}$$

In this study, the microchip is fabricated using a printed circuit board with a blue solder mask (substrate) and tin plating (electrodes). Since the surface plated with tin in an aqueous environment is too reflective and easily influenced by the light intensity, it is difficult to evaluate textures of the image for sharpness evaluation. In contrast, the blue substrate can be observed through the microscope (Fig.2(F)). Since the microscope at high magnification (20x) has a limited depth of field, sharp textures are become hard to detect if the microchip is not close enough. Therefore, a macro-micro detecting method is utilized for locating the microchip. The experiments showed that the sharpness value of the whole image may not be the highest even if the blue substrate is in focus, mainly due to the presence of tin electrodes from another layer. Therefore, the sharpness of the whole image is evaluated for coarse adjustment. After reaching the peak value, the area surrounding the electrode is defined as the local region and the sharpness value is also detected. The linear stage will be manipulated along the optical axis in both directions for fine adjustment. The stage will reposition at the height where the sharpness is the highest.

III. MATERIALS PREPARATION

To examine the pattern effect and the stability of the cell pattern, yeast cell was used in this study. Dry yeasts, Saccharomyces cerevisiae, were activated in sucrose solution with a concentration of $27g/L$ and heated for 1 hour at a temperature of 35 degrees Celsius. To test the pattern effect of the dead yeast cell, the solution containing the yeast cells was heated at a temperature of 90 degrees Celsius. Janus green B (Shanghai MAIKUN Chemical Co., Ltd) was used to stain dead yeast cells, enhancing the image contrast for viewing under the microscope. The cells were re-suspended in AHA (Ruibio) solutions at different concentrations for the experiments.

IV. RESULTS AND DISCUSSION

In large-scale cell patterning process, cells being patterned onto the substrate may not firmly be attached onto the surface, and they could be dissipated when the electric field is turned off. This problem could become more severe in a vigorous fluid flow environment. Besides, relative movement between the microchip and the substrate could induce disruptions in the channel. Therefore, a series of experiments were conducted to examine the effect of different experimental parameters on cell dissipation. First, the influences of the cell solution, including the cell concentration and the medium density, were examined. Then, the velocity of the moving stage on the cell dissipation was examined. Finally, a large-scale pattern was constructed on a glass substrate to demonstrate the feasibility and the performance of the automatic cell patterning system.

A. *Effect of cell concentration on cell cluster size*

During the cell patterning process, DEP forces are used to manipulate and concentrate cells towards the center and underneath the central electrode of the microchip, forming multiple cell clusters based on the design pattern. At a fixed channel height and voltage input, the size, or the diameter of the cell cluster is mainly dependent on the cell concentration of the medium. In this work, three concentrations, 2.5×10^6, 5×10^6, and 1×10^7 cells/mL were dispensed into the channel and an input voltage of $52V_{pp}$ was turned on for 2 minutes to allow the formation of cell clusters. Afterwards, the voltage

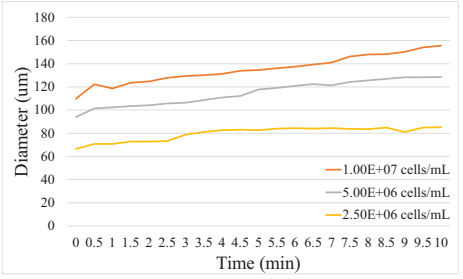

Fig. 3. Cell pattern dissipation rate with various concentration cell solution

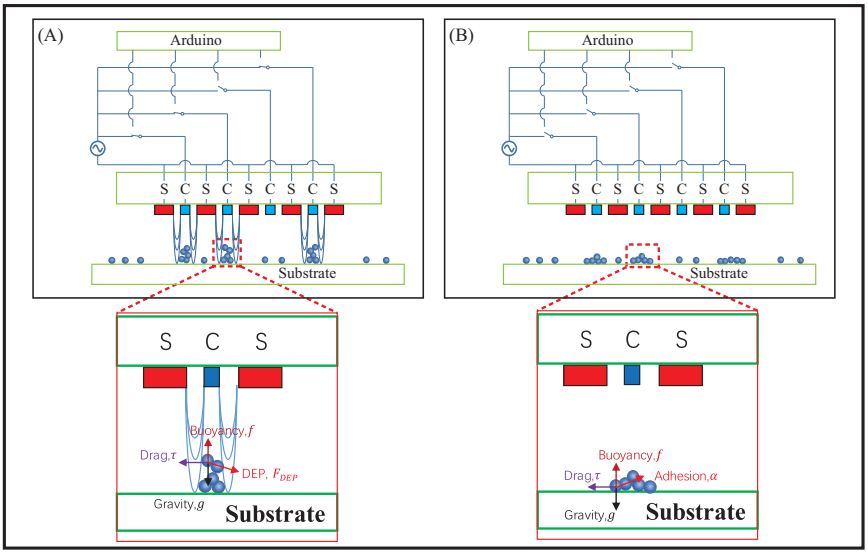

Fig. 4. The illustration of cell dissipation (A). when the electric field exist (B). after the electric field is cancelled

was turned off and the size of the clusters over time were measured, at a time interval of 30 seconds.

From the results shown in Fig.3, it can be observed that using a higher cell concentration can increase the initial cluster size from $65\mu m$ to $110\mu m$. This result indicates that a higher DEP force is induced on the cells due to a stronger dipole-dipole interaction between cells [16]. When the voltage is off, it can be observed that all cell clusters start to dissipate and the cell size continues to increase over time, to become $80\mu m$, and $160\mu m$, respectively. Using a medium with higher cell concentration, the size increases at a higher rate, and this can be explained as the accumulation of cells in the out-of-plane direction. Once the voltage is off, pyramid-like cell clusters start to collapse and spread out due to the gravity force (Fig.4). In order to minimize the distortion on the cell cluster, a lower cell concentration solution can be used to avoid spreading of excessive cells in the out-of-plane direction.

B. The cell dissipation influenced by the medium density

As discussed in the previous section, the cell clusters would gradually spread out in a steady environment. In addition to cell concentration, the cell dissipation rate is also influenced by the medium density. For a cell suspending in the medium, three forces, drag force, gravity force and buoyant force, are acting on the cell surface (shown in Fig.4). In the patterning procedure, cells are driven to group into clusters while holding in shape by DEP force. Meanwhile, there are also two interaction forces, between cell-to-cell and between cell-to-substrate, contributed for cell adhesion. Once the electric field is off, the adhesion force becomes the sole force against the fluid flow. The adhesion force is constituted of thousands of adhesion molecules and receptors on the cell surface [17], which can be modelled as a multi-point attachment model [18]. As the attachment area ($\boldsymbol{S}$) increases, more adhesion molecules are anchored and the adhesion force becomes larger ($\alpha \propto \boldsymbol{S}$).

When the cells are sunk to the bottom, the gravity force causes the stacked cells to flatten and deform, increasing the contact area to the substrate. This, in turn, helps to increase the adhesion force to hold the cell pattern in place. When the medium density is higher, the buoyant force produced from the medium increases, counteracting the gravity force to pull cells down to the substrate surface. In this work, AHA powder was added to change the medium density. According to the data from Flores-Rodriguez et at. [19], the relationship between the medium molecular concentration (B) and medium density (ρ) can be approximated with a linear polynomial function:

$$\rho(B) = 0.02922B + 0.998 \tag{4}$$

To explore the effect of the medium density, yeast cells ($\rho = 1.0725 g/cm^3$) are suspended in 0.2M AHA solu-

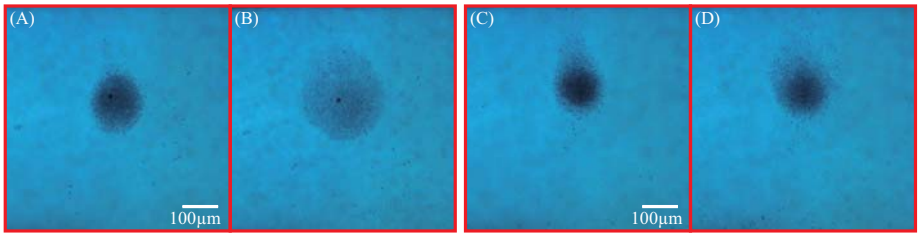

Fig. 5. Cell dissipation effect (A). in 0.6M AHA solution in the beginning of electric field cancelling (B). in 0.6M AHA solution after 10 minutes of electric field cancelling (C). in 0.2M AHA solution in the beginning of electric field cancelling (D). in 0.2M AHA solution after 10 minutes of electric field cancelling

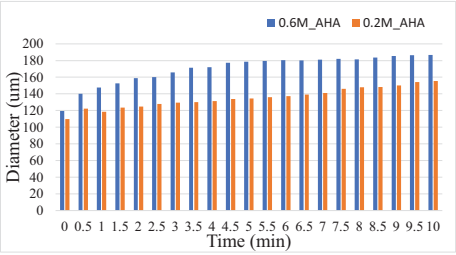

Fig. 6. Cell pattern dissipation effect in 0.2M and 0.6M AHA solution

tion ($\rho = 1.0038g/cm^3$) and 0.6M AHA solution ($\rho = 1.0155g/cm^3$) respectively with a cell concentration of 1×10^7 cells/mL. After 2 minutes of patterning, the voltage was turned off and the size of the cell cluster was measured over time. Fig.5 shows the pattern at the initial state and after 10 minutes. In the low-density environment (0.2M AHA Solution), it can be found that after 10 minutes, cells remain aggregated in a cluster form (Fig.5(C), (D)), as compared to that in the 0.6M AHA solution (Fig.5(A), (B)). Fig.6 shows the dissipation rate between 0.2M and 0.6M AHA solutions at different time. The cell pattern dissipates faster in a high-density solution, indicating that a low-density solution is preferable to retain the cell cluster.

It should be noted that the solution molarity not only increases the density, but also affect the medium relative permittivity. According to the cell model, the use of a high molarity AHA solution would increase the medium relative permittivity, thereby reducing the crossover frequency between p-DEP and n-DEP. Hence, an input frequency lower than 10MHz, which can be provided by general function generators, is sufficient to create n-DEP force. The simulation of the CM factor for yeast cells at different three mediums, namely, pure water ($\varepsilon_m = 78\varepsilon_0$), 0.4M AHA solution ($\varepsilon_m = 110\varepsilon_0$), 1M AHA solution ($\varepsilon_m = 160\varepsilon_0$), are shown in Fig.7. Meanwhile, the DEP force induced on the cells increase as well. From the findings, a moderate AHA concentration can be selected to balance between the required operating frequency and the dissipation rate of the cell cluster.

C. Selection on the stage velocity to minimize cell dissipation

In contrast to most of the microfluidic chips, this cell patterning system introduces a relative motion between the electrode and the substrate. As the substrate is moving at a velocity, u, it will create motions in the fluid that follow a linear velocity profile, in a channel with height, h, as shown

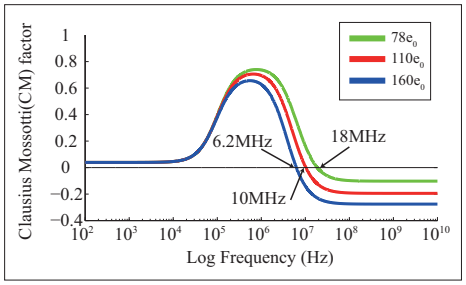

Fig. 7. Simulation of CM factor values for dead yeast cell in different AHA concentration solution with double-shell model at different frequencies

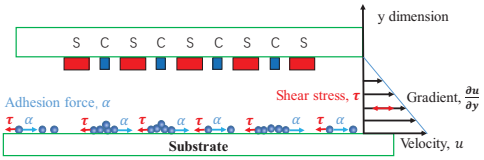

Fig. 8. Force analysis of cell with moving substrate

in Fig.8. At the boundary, a shear stress (τ) is induced, acting equally and oppositely on the fluid and on the substrate, with a differential relation:

$$\tau = \mu \frac{\partial u}{\partial y} \tag{5}$$

where μ is the viscosity of the medium.

To hold the cell firmly on the substrate, the shear force acting on the cells must be equal to or less than the adhesion force ($\tau \leq \alpha$). Therefore, the maximum velocity of the stage must satisfy the equation:

$$M \frac{V}{h}(2\pi r^2) = \alpha \tag{6}$$

where the velocity at the boundary is $\frac{u}{h}$ and the surface area of a half-spherical object is $2\pi r^2$.

To study the relationship between the moving stage and the cell spreading, an experiment was introduced to observe the cell pattern when the substrate on the stage was moving at different speeds. The diameter of the cell pattern was then recorded and shown in Fig.9. From the results, as the stage move at a higher speed, the constructed cell pattern dissipates at a higher rate, leading to a larger diameter. To minimize disruption to the pattern, the stage should be moved at a lower speed. Alternatively, calcium ions can be added to the solution to enhance the cell-cell adhesion and cell-substrate adhesion [20].

D. Multi-form patterning via the n-DEP

To examine the performance of the cell patterning system, a sequence of characters was constructed for characterization. Yeast cells at a concentration of 1×10^7 cells/mL were suspended in 0.2M AHA solution, and a glass substrate was mounted on the motorized stage of the microscope. A polymeric gasket was created to form a $30mm \times 20mm$ reservoir on the substrate surface, and the cell solution was filled into the reservoir. Then, the microchip was lower to immerse in the cell solution at $100\mu m$ above the glass substrate. Depending on the pattern, electrodes on the microchip were selectively powered on to create the cell pattern. After

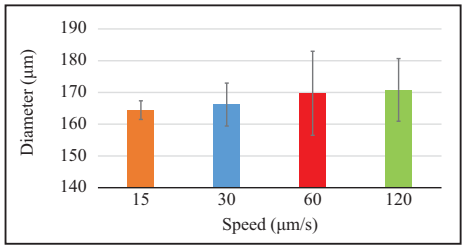

Fig. 9. Cell pattern dissipation with different stage velocities

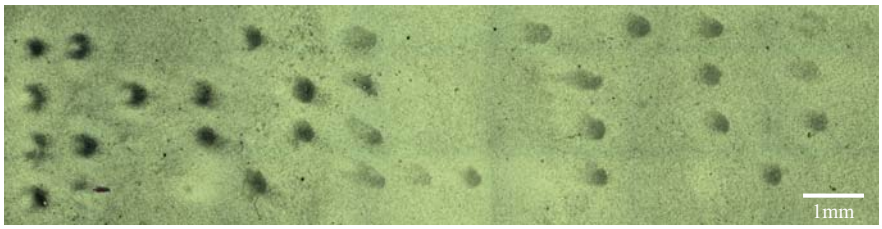

Fig. 10. A serial character pattern 'P', 'O', 'L', 'Y', 'U'

2 minutes of patterning, the signal was turned off and the substrate was displaced to a next position for patterning at a velocity of $480\mu m/s$. By repeating the procedures of patterning and substrate movement, a sequence of characters can be constructed on a single substrate. After patterning, calcium ions were added into the solution to enhance the cell adhesion on the substrate.

The pattern constructed from the cell patterning system is shown in Fig.10. Five characters "P", "O", "L", "Y", "U" are successfully formed on a glass substrate. As observed from the results, the quality of the first printed character, "U", is not as clear as the last character "P". The reason is due to gradual cell dissipation in a static environment over time. The total time required to print 5 characters is approximately 10.5 minutes. To minimize cell dissipation, the 2-minute used to pattern each character can be reduced or a larger microchip can be used to pattern multiple characters simultaneously.

V. CONCLUSION

In this study, a cell patterning system consisting of a height-adjustable microchip and a substrate on a movable stage was set up for the large-scale patterning. This microchip employed the n-DEP technique for non-contact cell patterning, and patterns were created on the substrate surface. Different parameters affecting the performance of the cell pattern were examined. Results show that a lower cell concentration and a lower medium density can help to reduce the cell spreading rate. The correlation between the channel height and the speed of the movable stage to the resultant pattern was also discussed. A large-scale pattern was successfully constructed for illustration. Comparing to traditional microfluidic channel for cell patterning, mounting the microchip on a linear stage can allow the channel height to be adjusted based on the application. In addition, the microchip can be programmed to generate different patterns. Combining with a movable stage, this system provides a simple and non-contact method with high flexibility to create large-scale cell patterns on various substrates to facilitate cell-based assay and characterization.

REFERENCES

[1] C. A. Vacanti, "History of tissue engineering and a glimpse into its future," *Tissue engineering*, vol. 12, no. 5, pp. 1137–1142, 2006.

[2] T. Yasukawa, K. Nagamine, Y. Horiguchi, H. Shiku, M. Koide, T. Itayama, F. Shiraishi, and T. Matsue, "Electrophoretic cell manipulation and electrochemical gene-function analysis based on a yeast two-hybrid system in a microfluidic device," *Analytical chemistry*, vol. 80, no. 10, pp. 3722–3727, 2008.

[3] D. R. Albrecht, R. L. Sah, and S. N. Bhatia, "Geometric and material determinants of patterning efficiency by dielectrophoresis," *Biophysical Journal*, vol. 87, no. 4, pp. 2131–2147, 2004.

[4] K. Ino, A. Ito, and H. Honda, "Cell patterning using magnetite nanoparticles and magnetic force," *Biotechnology and Bioengineering*, vol. 97, no. 5, pp. 1309–1317, 2007.

[5] J. El-Ali, P. K. Sorger, and K. F. Jensen, "Cells on chips," *Nature*, vol. 442, no. 7101, p. 403, 2006.

[6] H. A. Pohl, *Dielectrophoresis: The behavior of neutral matter in nonuniform electric fields (Cambridge Monographs on physics)*. Cambridge/New York: Cambridge University Press, 1978.

[7] K. Ino, H. Shiku, F. Ozawa, T. Yasukawa, and T. Matsue, "Manipulation of microparticles for construction of array patterns by negative dielectrophoresis using multilayered array and grid electrodes," *Biotechnology and bioengineering*, vol. 104, no. 4, pp. 709–718, 2009.

[8] B. Yafouz, N. A. Kadri, and F. Ibrahim, "The design and simulation of a planar microarray dot electrode for a dielectrophoretic lab-on-chip device," *International Journal of Electrochemical Science*, vol. 7, no. 12, pp. 12 054–12 063, 2012.

[9] N. Manaresi, A. Romani, G. Medoro, L. Altomare, A. Leonardi, M. Tartagni, and R. Guerrieri, "A cmos chip for individual cell manipulation and detection," in *Solid-State Circuits Conference, 2003. Digest of Technical Papers. ISSCC. 2003 IEEE International*. IEEE, 2003, pp. 192–487.

[10] M. Grad, A. W. Bigelow, G. Garty, D. Attinger, and D. J. Brenner, "Optofluidic cell manipulation for a biological microbeam," *Review of Scientific Instruments*, vol. 84, no. 1, p. 014301, 2013.

[11] K.-W. Huang, Y.-C. Wu, J.-A. Lee, and P.-Y. Chiou, "Microfluidic integrated optoelectronic tweezers for single-cell preparation and analysis," *Lab on a Chip*, vol. 13, no. 18, pp. 3721–3727, 2013.

[12] H.-y. Hsu, A. T. Ohta, P.-Y. Chiou, A. Jamshidi, S. L. Neale, and M. C. Wu, "Phototransistor-based optoelectronic tweezers for dynamic cell manipulation in cell culture media," *Lab on a Chip*, vol. 10, no. 2, pp. 165–172, 2010.

[13] L. Miccio, V. Marchesano, M. Mugnano, S. Grilli, and P. Ferraro, "Light induced dep for immobilizing and orienting escherichia coli bacteria," *Optics and Lasers in Engineering*, vol. 76, pp. 34–39, 2016.

[14] K. Huang, H. K. Chu, B. Lu, and L. Cheng, *Characterization of a Microchip Device for Cell Patterning via Negative Dielectrophoresis*, 2018 IEEE International Conference on Robotics and Biomimetics (ROBIO), Malaysia, 2018.

[15] Y. Huang, R. Holzel, R. Pethig, and X.-B. Wang, "Differences in the ac electrodynamics of viable and non-viable yeast cells determined through combined dielectrophoresis and electrorotation studies," *Physics in Medicine & Biology*, vol. 37, no. 7, p. 1499, 1992.

[16] M. Camarda, G. Fisicaro, R. Anzalone, S. Scalese, A. Alberti, F. La Via, A. La Magna, A. Ballo, G. Giustolisi, L. Minafra *et al.*, "Theoretical and experimental study of the role of cell-cell dipole interaction in dielectrophoretic devices: application to polynomial electrodes," *Biomedical engineering online*, vol. 13, no. 1, p. 71, 2014.

[17] K. V. Goossens and R. G. Willaert, "The n-terminal domain of the flo11 protein from saccharomyces cerevisiae is an adhesin without mannose-binding activity," *FEMS yeast research*, vol. 12, no. 1, pp. 78–87, 2012.

[18] J. Fu, H. Zhang, Z. Guo, D.-q. Feng, V. Thiyagarajan, and H. Yao, "Combat biofouling with microscopic ridge-like surface morphology: a bioinspired study," *Journal of The Royal Society Interface*, vol. 15, no. 140, p. 20170823, 2018.

[19] N. Flores-Rodriguez and G. H. Markx, "Improved levitation and trapping of particles by negative dielectrophoresis by the addition of amphoteric molecules," *Journal of Physics D: Applied Physics*, vol. 37, no. 3, p. 353, 2004.

[20] J. C. Bayly, L. M. Douglas, I. S. Pretorius, F. F. Bauer, and A. M. Dranginis, "Characteristics of flo11-dependent flocculation in saccharomyces cerevisiae," *FEMS yeast research*, vol. 5, no. 12, pp. 1151–1156, 2005.